African Journal of Mathematics and Computer Science Research Vol. 2(7), pp. 157-162, August, 2009
Available online at http://www.academicjournals.org/AJMCSR
© 2009 Academic Journals

Full Length Research Paper

Modeling laminar flow between a fixed impermeable disk and a porous rotating disk

D. P. Kavenuke[1]*, E. Massawe[1] and O. D. Makinde[2]

[1]Mathematics Department, University of Dar es Salaam, P. O. Box 35062, Tanzania.
[2]Applied Mathematics Department, University of Limpopo, Private Bag X1106, Sovenga 0727, South Africa.

Accepted 19 March, 2009

We formulate a mathematical model that governs operations of many engineering systems particularly the ceiling fan to explain the fluid flow between the fixed impermeable and the porous rotating disks. The model is based on the continuity and the Navier-Stokes equations which are reduced into a set of coupled ordinary differential equations through transformation by similarity variables. The coupled ordinary differential equations are solved using perturbation techniques and the series solution obtained is improved by Paté's approximation. Our results meet the supposition that, with laminar flow regime, suction increases with increasing speed of rotation of the rotating porous disk and these are shown on the graphical representations.

Key words: Impermeable disk, laminar flow, porous rotating disk, shear stress, Padé approximation.

INTRODUCTION AND MODEL FRAMEWORK

The problem of laminar flow between two parallel disks stemming from both practical interests (example, ocean circulation models and turbo machinery applications) and theoretical interests (example, exact solutions of the Navier-Stokes equations in certain geometric limiting cases) has received much attention over the years (Lopez, 1996). In modern times, the theory of flow through convergent–divergent channels has many applications in aerospace, chemical, civil, environmental, mechanical and bio-mechanical engineering as well as in understanding rivers and canals (Makinde and Mhone, 2006). Due to the complexity of a real fluid flow, certain assumptions are made to simplify the mathematical convenience. Some of the basic assumptions are; the fluid is ideal (that is, without viscosity for mathematical convenience). In situations where the effect of viscosity is small, this assumption often yields results of acceptable accuracy, although where viscosity plays a major part (example, in boundary layers), the assumption is clearly untenable. The flow is steady (that is, the flow parameters do not change with time). The fluid is incompressible (or has constant density) (Massey, 1989).

We consider the flow between a fixed impermeable disk and a porous rotating disk (Figure 1) both being immersed in a large body of fluid. Motion of the fluid is induced by the rotation of the porous disk. This study is interesting in its own right and also based on its applicability.

In the sequel, the following notation will be used:

$L :=$ Distance between the two disks.
$r :=$ Radius of each disk
$\Omega :=$ Angular speed of the rotating disk
$\varepsilon :=$ Measure of the angular speed or momentum of the rotating porous disk
$W :=$ Suction velocity at which fluid is withdrawn from the rotating disk (injection if W is negative).
$u, v, w :=$ Velocity components in the directions $r, \theta,$ and z respectively.

f, g, P are the similarity variables used to reduce the Navier-Stokes non-linear partial differential equations into a system of non-linear ordinary differential equations. For fixed impermeable disk, $u = 0, w = 0, v = 0$ while for porous rotating disk, $u = 0, w = W, v = r\Omega\varepsilon$. The disks are separated by a distance L which is small compared to their radii.

The direction of fluid flow as shown by the arrows in the Figure 1 is heading towards the porous disk which is rotating with a constant angular speed Ω. The suction velocity is assumed to be constant and equal to W. The

*Corresponding author. E-mail: kavenuke@maths.udsm.ac.tz, kavedasi@yahoo.co.uk.

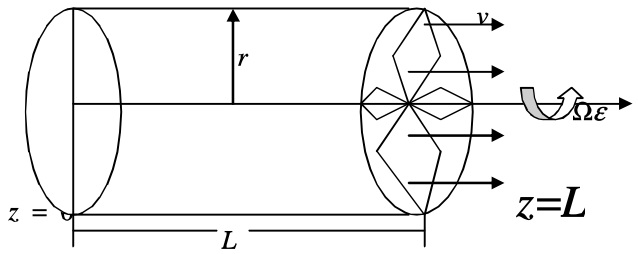


Figure 1. Physical model representing laminar flow between parallel disks.

rotation speed is given by $\Omega\varepsilon$, where Ω is the angular speed of the rotating disk and the parameter ε is a regulator which controls rotation of the disk $(0 \le \varepsilon \le 1)$. If $\varepsilon = 0$, then there is no rotation but for $\varepsilon > 0$, rotating occurs.

The question of existence and uniqueness of solutions in the similarity formulation has been raised (Mellor et al., 1968; Parter, 1982). Moreover, a question on the behaviour of the flow between the two disks and in particular near the stationary disk as the speed of the rotating disk approaches infinity has not been satisfactorily addressed in this type of formulation.

The nature of the flow between the two disks with finite radii is also not yet known.

There are arguments that boundary layers are formed on both disks with the interior fluid rotating (Batchelor, 1951) whereas on the other hand, the boundary layers are formed only on the rotating disk with the interior being essentially stationary (Stewartson,1953).

Fluid flow is either turbulent or laminar. Turbulence involves entirely haphazard motions of small fluid particles in all directions and it is impossible to follow the adventures of every individual particle. With laminar flow, the individual particles of fluid follow paths that do not cross those of neighbouring particles. Herein, the flow is assumed to be laminar. A brief comment on previous works provides the context of this paper.

The problem of flow over a rotating disk has a long history, originally describing similarity transformations that enable Navier-Stokes equations to be reduced to a system of coupled ordinary differential equations (Von Karman, 1921). Flows between or above infinite rotating disks are known as the generalized Von Karman swirling flows. Ever since Von Karman derived the simplified equations that govern the flow over an infinite rotating disk, this problem has attracted many researchers (Greenspan, 1968; Lopez, 1996; Owen and Wilson, 2000; Mellor et al., 1968; Kuiken, 1971; Kelson et al., 2000 to name but a few). Theoretical work on this class of flows has been undertaken mainly in the framework of similarity solutions because the assumption of self-similarity to reduce Navier-Stokes equations from partial to ordinary differential equations greatly simplifies the analysis. Lopez (1996) studied the flow between a stationary and a rotating disk shrouded by a co-rotating cylinder. He used a numerical treatment of the axi-symmetric Navier-Stokes equations together with some experiments for the case of finite stationary and rotating disks bounded by a co-rotating sidewall and found that in the long time limit, the solutions are steady and essentially self-similar.

MODEL AND ANALYSIS

Figure 1 depicts a system of porous rotating disk and a stationary disk both being immersed in a large fluid body. Fluid motion is set up by both rotation of the porous disk and suction (or injection) of the fluid itself.

We use the cylindrical polar coordinates (r, ϕ, z) and denote the corresponding velocity components by (u, v, w). However, the angle ϕ will not appear in our analysis because of rotational symmetry. The plane $z = L$ rotates about the $z-$axis with constant angular velocity $\Omega\varepsilon$ and the suction velocity is given by W.

In order to neglect the end effects, we assume that the gap L is very small compared to the radii of the disks, that is, $L << r$ $(0 < L << r)$.

The equations governing the motion of an incompressible viscous fluid arise from conservation of mass principle and the momentum principle.

From the conservation of mass principle, we have:

$$\frac{1}{r}\frac{\partial}{\partial r}(ru) + \frac{\partial w}{\partial z} = 0 \tag{1}$$

From the momentum principle and ignoring gravity, we have the Navier-Stokes equations, one for each co-ordinate direction:

$$u\frac{\partial u}{\partial r} + w\frac{\partial w}{\partial z} - \frac{v^2}{r} = -\frac{1}{r}\frac{\partial p}{\partial r} + \upsilon\left[\frac{\partial^2 u}{\partial r^2} + \frac{\partial}{\partial r}\left(\frac{u}{r}\right) + \frac{\partial^2 u}{\partial z^2}\right] \tag{2}$$

$$u\frac{\partial v}{\partial r} + w\frac{\partial v}{\partial z} + \frac{uv}{r} = \upsilon\left[\frac{\partial^2 v}{\partial r^2} + \frac{\partial}{\partial r}\left(\frac{v}{r}\right) + \frac{\partial^2 v}{\partial z^2}\right] \tag{3}$$

$$u\frac{\partial w}{\partial r} + w\frac{\partial w}{\partial z} = -\frac{\partial P}{\partial z} + \upsilon\left[\frac{\partial^2 w}{\partial r^2} + \frac{1}{r}\frac{\partial w}{\partial r} + \frac{\partial^2 u}{\partial z^2}\right] \tag{4}$$

Boundary conditions and equations in similarity variables

The small gap L between the two disks allows us to neg-

lect the behaviour of the flow around the edges. Therefore, the boundary conditions to be specified are those applicable to velocity components at both disk surfaces and not the edges.

For the velocity, it is assumed that the no-slip condition applies at the surface of the disks.

On the fixed disk, $z=0$, the no-slip conditions are $u(r,0)=0$, $v(r,0)=0$ and $w(r,0)=0$. On the rotating disk, $z=L$, the no-slip conditions are $u(r,L)=0, v(r,L)=r\Omega$ and because of fluid suction on the disk, the axial velocity is given by $w(r,L)=\varepsilon W$.

Since the fluid is incompressible, it is possible to define the stream function from the governing continuity equation in two dimensions. This enables us to solve the continuity equation (2) in the familiar way by setting

$$u=\frac{1}{r}\frac{\partial\Psi}{\partial z}, w=-\frac{1}{r}\frac{\partial\Psi}{\partial r} \tag{5}$$

and by defining a dimensionless normal distance from the disk (Von Karma),

$$\eta=\frac{z}{L}=\frac{\Omega z}{W} \quad . \tag{6}$$

We assume a similarity transformation of the form

$$\Psi(r,\eta)=r^2 f(\eta)W \tag{7}$$

Equations (5) and (7) yield the expression for the radial and tangential velocities

$$u=r\Omega f'(\eta) \quad , \quad w=-2Wf(\eta) \tag{8}$$

For the axial velocity and pressure variables, we assume that

$$v=r\Omega \mathrm{g}(\eta) \quad , \quad \mathrm{p}=-\frac{1}{2}\rho r^2 A\Omega^2+\rho P(\eta) \tag{9}$$

The corresponding boundary conditions for the functions f and g are

$$f'(0)=0, \quad f(0)=0, \quad \mathrm{g}(0)=0, \quad f'(1)=0 \quad ,$$
$$f(1)=-\frac{1}{2}, \quad \mathrm{g}(1)=\varepsilon .$$

Substituting (8) and (9) into equations (2)-(4), we obtain

$$f'(\eta)^2-2f(\eta)f''(\eta)-\mathrm{g}^2(\eta)=A+\frac{1}{R_e}f'''(\eta) \tag{10}$$

$$2\left(f'(\eta)\mathrm{g}(\eta)-f(\eta)\mathrm{g}'(\eta)\right)=\frac{1}{R_e}\mathrm{g}''(\eta) \tag{11}$$

$$P'(\eta)=-4W^2 f'(\eta)f(\eta)-\frac{2Wv}{L^2}f''(\eta) \tag{12}$$

Where the primes denote differentiation with respect to η, the parameter $R_e=\frac{W^2}{\Omega v}$ is the Reynolds number and A is an arbitrary constant. Differentiating (10) with respect to η, we obtain:

$$-2\left(ff'''+\mathrm{g}'\mathrm{g}\right)=\frac{1}{R_e}f'''' \tag{13}$$

Equation (11) can be written as

$$2\left(f'\mathrm{g}-f\mathrm{g}'\right)=\frac{1}{R_e}\mathrm{g}'' \tag{14}$$

Our main focus is on solving the two coupled nonlinear ordinary differential equations (13) and (14) subject to the boundary conditions:

$$f'(0)=0, \quad f(0)=0, \quad \mathrm{g}(0)=0, \quad f'(1)=0 \quad ,$$
$$f(1)=-\frac{1}{2}, \quad \mathrm{g}(1)=\varepsilon .$$

Though the transformation has provided a set of ordinary differential equations, a closed form solution is still not possible. Consequently, we apply the perturbation technique (Makinde, 1999) and obtain a result similar to that of Kelson and Desseaux (2000). Treating R_e as a perturbation parameter, substituting the expansions

$$f=\sum_{i=0}^{\infty}R_e^{\,i}f_i \quad , \quad \mathrm{g}=\sum_{i=0}^{\infty}R_e^{\,i}\mathrm{g}_i$$

into equations (13) and (14) transforms the intractable original problem into a sequence of simple ones. By collecting terms of the same order, we have:

$$f_0''''=0 \quad , \quad \mathrm{g}_0''=0, \tag{15}$$

subject to the boundary conditions

$$f'(0)=0, \quad f(0)=0, \quad \mathrm{g}(0)=0, \quad f'(1)=0,$$

$$f(1) = -\frac{1}{2}, \quad g(1) = \varepsilon .$$

The solution of (15) under the given boundary conditions yields the following

$$f_0 = \eta^3 - \frac{3}{2}\eta^2 , \; g_0 = \varepsilon\eta$$

Thus, the perturbed solutions (Makinde, 1996) of the system of ordinary differential equations (13) and (14) takes the forms

$$f(\eta,\varepsilon) = f_0(\eta,\varepsilon) + R_e f_1(\eta,\varepsilon) + R_e^{\,2} f_2(\eta,\varepsilon) + \ldots$$
$$g(\eta,\varepsilon) = g_0(\eta,\varepsilon) + R_e g_1(\eta,\varepsilon) + R_e^{\,2} g_2(\eta,\varepsilon) + \ldots$$

where f_i and g_i for $i = 0$, 1, 2, ... are computed using MAPLE.

Fluid pressure distribution

From equation (12), we have

$$\frac{\partial p}{\partial \eta} = -4W^2 f'(\eta) f(\eta) - \frac{2Wv}{L} f''(\eta), \qquad (16)$$

Integrating the above equation and applying the boundary conditions, we obtain

$$P(r,\eta) - P(r,0) = -2W^2\left(f(\eta)^2 - f(0)^2\right) - \frac{2Wv}{L}\left(f'(\eta) - f'(0)\right) \qquad (17)$$

$$P^* = \frac{P(r,\eta) - P(r,0)}{2W^2} = f(\eta)^2 + \frac{1}{R_e} f'(\eta) \qquad (18)$$

Wall shear stress

The action of velocity in the fluid adjacent to the disks tends to set a tangential shear stress which opposes the rotation of the disk. The tangential stresses at the rotating porous disk are given by

$$\tau_{\theta z} = \frac{\mu \partial v}{\partial z} = \frac{\mu r \Omega^2}{W} g'(1) \qquad (19)$$

$$\tau_{zr} = \frac{\mu \partial u}{\partial z} = \frac{\mu r \Omega^2}{W} f''(1) \qquad (20)$$

Thus, we need to obtain the series for $g'(1)$ and $f''(1)$ from our previous series solution of f and g above. Using computer symbolic algebra package (MAPLE), we have obtained the first 22 terms of the solution series for several values of the rotating disk parameter ε for

$$g'(1) = \sum_{i=0}^{n} a_i R_e^{\,i} , \qquad f''(1) = \sum_{i=0}^{n} b_i R_e^{\,i}$$

The well-known Padé approximation over the last few years, proved itself as a powerful benchmarking tool and a potential alternative to traditional numerical techniques in various applications in sciences and engineering (Makinde, 2006).

This semi-numerical approach is also extremely useful in the validation of purely numerical scheme. In order to improve on the above series solution, we therefore employ this approximation.

The wall shear stresses at the rotating disk is given by

$$\tau_{\theta z} = \frac{\mu r \Omega^2}{W} g'(1) \qquad (21)$$
$$= -2W^2 f(\eta)^2 - \frac{2Wv}{L} f'(\eta) , \quad \text{since}$$
$$f(0) = f'(0) = 0$$

Hence, the expression for the pressure drop in the axial direction in non-dimensional form is given by

$$\tau_{zr} = \frac{\mu r \Omega^2}{W} f''(1) \qquad (22)$$

Where $g'(1) = \sum_{n=0}^{\infty} a_n R_e^{\,n}$, $f''(1) = \sum_{n=0}^{\infty} b_n R_e^{\,n}$.

The series for the porous rotating disk wall shear stress is transformed as follows of the denominator of the fraction. After transforming the solution series into several diagonal Padé approximants [M/M] and analyzing the denominators of the resulting double series, we observed that a singularity occurs at a value of suction, Reynolds number Re ≈ 6.2 which may vary slightly above this value depending on the choice of $0 < \varepsilon \leq 1$, the parameter determining the rotational speed of the porous disk.

RESULTS AND DISCUSSION

Insight into the physical occurrences within the flowing fluid can be obtained by a study of the velocity profiles. The distributions of the normal velocity w, radial velocity u and azimuthal velocity v are plotted as a func-

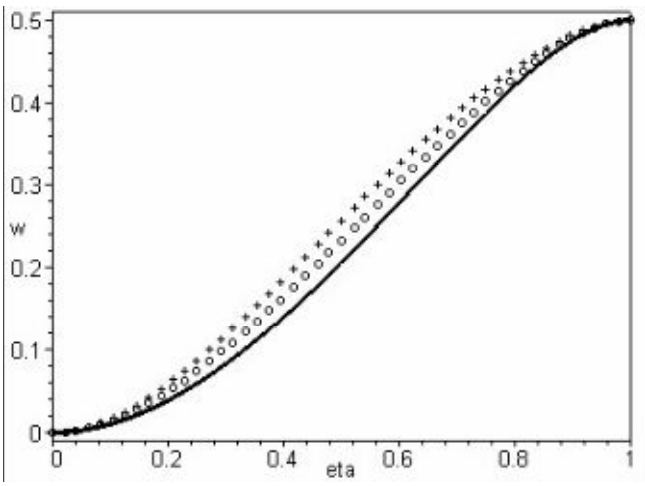


Figure 2. Normal velocity profile, Re=6.0: (__) ε=0.3; (ooo) ε = 0.5 and (+++) ε =1.0.

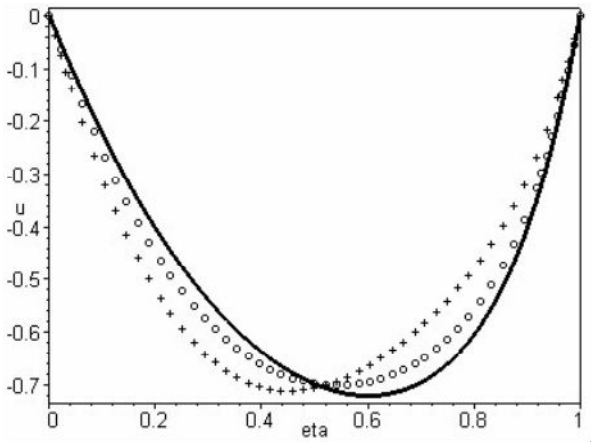


Figure 3. Radial velocity profile, Re=6.0: (__) ε =0.3; (ooo) ε = 0.5 and (+++) ε =1.0.

tion of eta (η). Also, the pressure and shear stress variations are represented graphically.

Normal velocity profile with constant Reynolds number

In the sequel, we shall use the symbols: (___) to represent the solid lines while (ooo) and (+++) will represent the other two lines in the figures.

From equation (8), $w = -2Wf(\eta)$. The normal velocity w is expressed in terms of $-f(\eta)$ Note that w is plotted against η while fluid suction at the porous rotating disk is constant being fixed at $R_e = 6.0$. In this case, rotation of the porous disk is not constant. It varies in the increasing manner and this is exemplified by ε- values that increase from 0.3 to 1.0. Figure 2 shows that the fluid

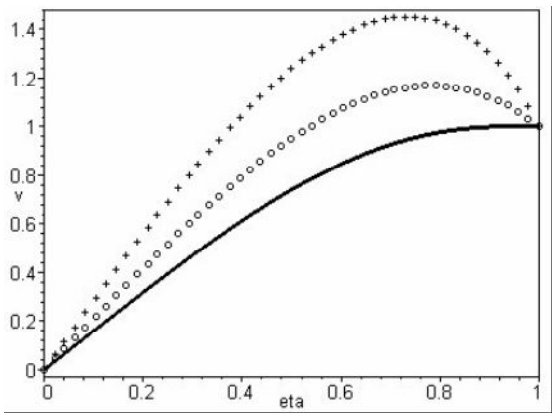


Figure 4. Azimuthal velocity profile for ε =1.0: (__) Re =4.0; (ooo) Re= 5.0 and (+++) Re=6.0

normal velocity (w) increases transversely towards the rotating porous disk. A further increase in this trend is observed with an increase in the speed of the porous disk rotation.

Radial velocity profile with constant Reynolds number

From equation (8) $u = r\Omega f'(\eta)$, where the radial velocity u is expressed in terms of $f'(\eta)$. In this case, u is plotted against η, fluid suction being kept constant at $R_e = 6.0$. Rotation of the porous disk is not constant and varies in the increasing manner as indicated by ε- values that increase from 0.3 - 1.0. A pattern of radial velocity profile is also observed in Figure 3. An increase in the speed of the rotating porous disk causes a further fluid inflow near the rotating disk but less fluid inflow near the fixed impermeable disk.

Azimuthal velocity profile with constant rotation parameter

From Equation (9), $v = r\Omega g(\eta)$. The azimuthal velocity v is expressed in terms of $g(\eta)$ and its profile is shown below.

v is plotted against η while the speed of rotation of the rotating disk is fixed at $\varepsilon = 1.0$. Suction is kept on increasing as shown by the increase of Reynolds numbers from left to right. The azimuthal velocity increases transversely towards the rotating porous disk. The maximum azimuthal velocity is observed at a distance very close to the rotating disk but not at the rotating disk itself. It is further observed that an increase in the suction Reynolds numbers causes a further increase in the azimuthal fluid velocity. The Azimuthal velocity profile is depicted in Figure 4.

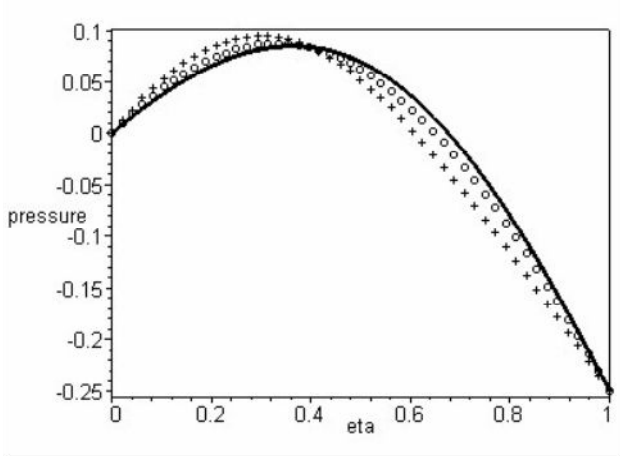


Figure 5. Fluid pressure distribution: Re=6.0: (__) ε =0.3; (ooo) ε = 0.5 and (+++)ε =1.

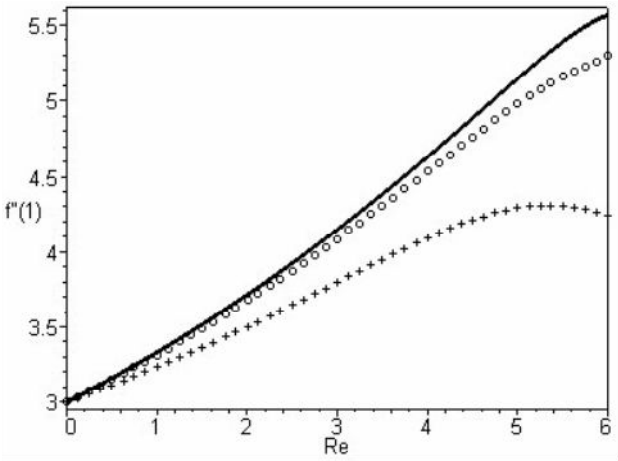


Figure 6. Shear stress at the rotating porous disk due to radial velocity: (__) ε =0.3; (ooo) ε = 0.5 and (+++)ε =1.0.

Fluid pressure distribution with constant suction

In this case, the pressure is plotted against η while suction is constant ($R_e = 6.0$). The speed of rotation of the porous rotating disk varies in the increasing sense as shown by the increase in the ε- values from 0.3 - 1.0. Fluid pressure increases from the fixed impermeable disk towards the porous rotating disk reaching its maximum value at a distance close to the impermeable disk and drops gradually towards the porous rotating disk due to suction. An increase in the speed of rotation of the porous rotating disk causes a further decrease in the pressure drop towards the rotating porous disk. Figure 5 depicts the fluid pressure distribution.

Shear stress at the rotating porous disk due to radial velocity on its wall

This is expressed in terms of $f''(1)$. $f''(1)$ is plotted against R_e while rotation of the porous disk is constantly increasing (i.e. $\varepsilon \to 1.0$). The plot is indicated in Figure 6 which shows that radial shear stress increases with increase in suction. Moreover, an increase in the speed of rotation of the porous rotating disk causes a decrease in the radial shear stress with increase in suction.

Conclusion

The presence of fluid inflow between the two disks guarantees the absence of cooling and in general, cooling is felt outside the region and in front of the porous rotating disk due to suction and fluid outflow. This effect can easily be observed from a ceiling fan operation and other fan systems used in our homes.

For this particular problem, the numerical analysis shows that there is a singularity at $R_e \approx 6.2$. This singularity can be regarded as a property of the exact solution for the problem. $\varepsilon = 0$ corresponds to the case of flow between an impermeable fixed disk and a non-rotating porous disk.

REFERENCES

Batchelor GK (1951). "Note on a class of solutions of the Navier-Stokes equations representing steady rotationally-symmetric flow". Q. J. Mech. Appl. Math. 4: 29.
Greenspan HP (1968). The Theory of Rotating Fluids. Cambridge University Press, Cambridge.
Kelson N, Desseaux A (2000). "Note on porous rotating flow". ANZIAM J. 42: 837-855.
Kuiken HK (1971). "The effect of normal blowing on the flow near a rotating disk of infinite extent", J. Fluid Mech. 471(4): 789-798.
Lopez JM (1996). "Flow between a stationary and a rotating disk shrouded by a co-rotating cylinder". Phys. Fluids. 8:10.
Makinde OD (1996). Computer Extension and bifurcation study by analytic continuation of porous tube flow. J. Math. Phys. Sci. 30: 1-24.
Makinde OD (1999). Extending the utility of perturbation series to problems of laminar flow in a porous and a diverging tube, J. Australian. Math. Soc. Series B. 41: 118-128.
Makinde OD (2006). Thermal ignition in a relative viscous flow trough a channel filled with porous medium, J. Heat. Transf. 128: 601-604.
Makinde OD, Mhone PY (2006). Hermite-Padé approximation approach to MHD Jeffery-Hamel Flows. Appl. Math. Comput.181(2): 966-972.
Massey BS (1989). Mechanics of Fluid. Chapman and Hall Ltd, London.
Mellor GL, Chappel PJ, Stokes VK (1968). "On the flow between a rotating and a stationary disk". J. Fluid Mech. 31(1): 95-112.
Owen JM, Wilson M (2000). "Some current research in rotating-disk systems"http://www.ichmt.org/abstracts/Turbine2000/abstracts/13.pdf
Parter SV (1982). "On the swirling flow between rotating coaxial disks: A survey. Theory and Applications of singular Perturbation", W. Eckhaus, E.M. de Jager (eds), Springer-Verlag, Berlin, Heidelberg, New York.Lecture Notes in Mathematics 942: 258.
Stewartson K (1953). On the flow between two rotating coaxial disks, Proc.Cambridge Philos. Soc. 49: 333.
Von Karman T (1921). Laminar und turbulente reibung. Z. Angew. Math 1: 233-252.